High Energy Density Physics 23 (2017) 1–5

Contents lists available at ScienceDirect

High Energy Density Physics

journal homepage: www.elsevier.com/locate/hedp

Accretion shocks in the laboratory: Design of an experiment to study star formation

R.P. Young[*,a], C.C. Kuranz[a], R.P. Drake[a], P. Hartigan[b]

[a] University of Michigan, Department of Climate and Space Sciences and Engineering, 2455 Hayward St., Ann Arbor, MI 48109, USA
[b] Rice University, Physics and Astronomy Department, 6100 Main MS-61, Houston, Texas 77005, USA

ARTICLE INFO

Article History:
Received 29 August 2016
Accepted 16 January 2017
Available online 13 February 2017

Keywords:
Laboratory astrophysics
Star formation
Accretion
Shocks
Jets

ABSTRACT

We present the design of a laboratory-astrophysics experiment to study magnetospheric accretion relevant to young, pre-main-sequence stars. Spectra of young stars show evidence of hotspots created when streams of accreting material impact the surface of the star and create shocks. The structures that form during this process are poorly understood, as the surfaces of young stars cannot be spatially resolved. Our experiment would create a scaled "accretion shock" at a major (several kJ) laser facility. The experiment drives a plasma jet (the "accretion stream") into a solid block (the "stellar surface"), in the presence of a parallel magnetic field analogous to the star's local field. We show that this experiment is well-scaled when the incoming jet has $\rho \sim 10^{-6}$–10^{-5} gcm^{-3} and $u \sim 100$–200 kms^{-1} in an imposed field of $B \sim 10$ T. Such an experiment would represent an average accretion stream onto a pre-main sequence star with $B \sim 700$ G.

1. Introduction

Accretion shocks form when material from an accretion disk impacts at the surface of the object growing at its center. The object's magnetic field governs the interaction between the two through what it called magnetospheric accretion. Originally proposed by Königl [22], who extended the compact object work of Ghosh and Lamb [8,9] to T Tauri stars (low-mass pre-main-sequence stars), the magnetospheric accretion model has material from the accretion disk lifted out of the plane of the disk and "funneled" along the star's magnetic field lines to its surface. Today, there is ample evidence that magnetospheric accretion occurs on T Tauri stars (see Bouvier et al. [3] and references therein). There is also evidence of magnetospheric accretion occurring on T Tauri stars' more massive counterpart, Herbig Ae/Be stars [12,29,31].

When the supersonic material impacts the surface of the young star—T Tauri or Herbig Ae/Be—an accretion shock hot enough to emit soft X-rays ($T \sim 10^6$–10^7 K) forms. There is ample evidence of this in the X-ray spectra of T Tauri stars [1,2,4,13,21,38,42,43], and evidence is growing that at least some Herbig Ae/Be stars exhibit X-ray-emitting accretion shocks as well [6,10,44,45].

The mass accretion rate of a star ($\dot{M}$, usually on the order of $10^{-8} M_\odot$ per year) can be determined from the effect that these X-ray emitting accretion shocks have on the star's spectrum. The X-rays heat the surrounding photosphere, producing spots of hot plasma [5]. Compared to a similar non-accreting star, an accreting star ought to have excess emission in the optical and UV due to these spots, and its accretion rate can be calculated from the amount of excess emission [15,16,30,33,46].

However, these accretion rate calculations are only as good as the understanding of accretion shock structure behind them. Because the surfaces of young stars cannot be spatially resolved, the structure of accretion shocks has not been directly studied. For example, do accretion shocks penetrate the star's photosphere, potentially hiding much of the accretion shock's energy from observers? Or, do accretion shocks create large "splashes" when they hit the surface of the star, making it appear the shock covers more surface area than it actually does? Either of these scenarios would potentially change the calculated accretion rate significantly.

Simulations of accretion shocks have largely served to underscore how complicated and inherently three-dimensional the systems are. Three-dimensional simulations by Romanova et al. [39] predict that accretion hotspots should be inhomogenous and irregularly shaped. Likewise, simulations by Orlando et al. [34] found that T Tauri accretion shocks can produce violent splash zones, particularly when the magnetic field strength is too low to contain the accretion shock.

To this end, we propose our design of an experiment to produce a scaled laboratory version of an accretion shock. We would use a high-energy (several kJ) laser to make a supersonic plasma jet (the "accretion stream") and drive it into a solid block (the "stellar surface") in the presence of an imposed magnetic field. Section 2 establishes the connection between magnetic accretion on a

* Corresponding author.
E-mail address: rachelpierson@gmail.com (R.P. Young).

http://dx.doi.org/10.1016/j.hedp.2017.01.004
1574-1818/

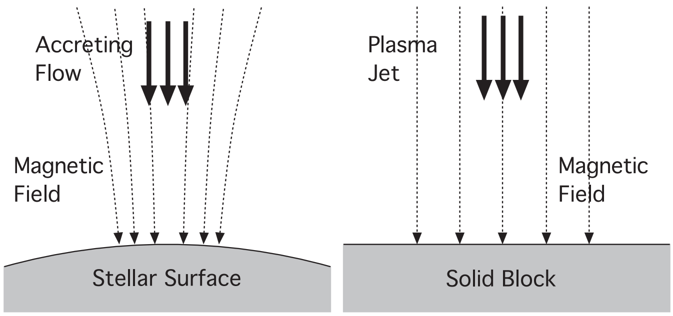

Fig. 1. In the astrophysical system (left), accreting plasma falls to the stellar surface along magnetic field lines (depicted here as a magnetic dipole at the pole of the star). In the lab experiment (right), a plasma jet collides with a solid block with a parallel background magnetic field.

pre-main-sequence star and the laboratory experiment and lays out the plasma parameters that we must seek to have a well-scaled experiment. Section 3 discusses design considerations of our experiment, and Section 4 presents our conclusions.

2. Experimental goals

2.1. Basic configuration

Laboratory astrophysics offers the ability to probe scaled astrophysical systems in an experimental setting [36,37,41]. Examples of such experimental campaigns include the work of Kuranz et al. [25], who created Rayleigh–Taylor blast waves relevant to supernovae remnants; the work of Hartigan et al. [14], who created deflected supersonic jets relevant to Herbig–Haro objects; and the work of Krauland et al. [23], who created reverse shocks relevant to interacting binaries.

Our astrophysical system, an accreting young star, consists of (1) accreting material which collides with (2) the surface of the growing star in the presence of (3) a magnetic field parallel to the material's flow and perpendicular to the star's surface. Creating a scaled version of this system means translating these three into the lab, as seen in Fig. 1. In the experiment, we drive a plasma jet (the "accreting material") into a solid block (the "stellar surface") with an imposed magnetic field.

2.2. Dimensionless numbers

Astrophysical systems can never be scaled and reproduced perfectly in the lab. Having a worthwhile experiment, therefore, hinges on discerning which physical processes are most important and translating them into an experiment appropriately. Ryutov et al. [41] lays out a theoretical basis for doing so: one must ensure that dimensionless numbers (for example, Reynolds number) that define the system are at least in similar regimes.

There are five dimensionless numbers that concern the accretion shock experiment. The first two determine whether a shock can form in the first place, the second two determine the role of magnetic fields in the experiment, and the last is the Reynolds number, which relates the importance of viscosity in the system. The scaling criteria we impose are as follows:

1. $\mathcal{M} > 1$. $\mathcal{M}$ is the Mach number, the ratio of the flow velocity of the jet to the speed of sound inside the jet; we need a supersonic jet in order to have a shock. Sound speed was calculated according to

$$c_s = 9.79\times10^5\sqrt{\frac{\gamma(Z+1)T_e}{A}}\,\mathrm{cm\,s^{-1}}, \tag{1}$$

where γ is the adiabatic index, Z is the ionizations, T_e is the temperature in eV, and A is the atomic mass in proton masses.

2. $\lambda_{\mathrm{MFP}} < L$. λ_{MFP} the ion-ion mean free path inside the plasma and L is the overall lengthscale of the experiment. We impose $\lambda_{\mathrm{MFP}} < L$ in order to observe a shock in the experiment.
Mean free path was calculated according to

$$\lambda_{\mathrm{MFP}} = \frac{1}{n_i\sigma_{90}^{ii}4\ln\Lambda_{ii}}, \tag{2}$$

where n_i is the ion density, σ_{90}^{ii} is the 90° cross-section, and $\ln\Lambda_{ii}$ is the ion-ion Coulomb lambda. The 90° cross-section was calculated according to

$$\sigma_{90}^{ii} = \frac{\pi e^4 Z^4}{m_i u^4}, \tag{3}$$

where e is the charge of an electron, Z is the average ionization, m_i is the ion mass, and u is the relevant velocity (in this case the flow velocity).
This criterion ($\lambda_{\mathrm{MFP}} < L$) also ensures that our plasma is collisional. Park et al. [35] give the condition for a collisionless plasma as $L \ll \lambda_{\mathrm{MFP}}$, where λ_{MFP} is the ion-ion MFP of the heaviest ion species, so a plasma with $\lambda_{\mathrm{MFP}} < L$ would be collisional.

3. $\ell_M < L$. ℓ_M is the magnetic diffusion lengthscale, and L is the overall lengthscale of the experiment. We impose $\ell_M < L$ in order to ensure the magnetic field does not diffuse away during the experiment. To find ℓ_M, we consider a generic diffusion equation,

$$\frac{\partial\phi}{\partial t} = D\nabla^2\phi, \tag{4}$$

where ϕ is some generic diffusing quantity and D is the generic diffusion constant with units L^2T^{-1}. Applying unit analysis we find

$$\frac{\phi}{\tau} = D\frac{\phi}{\ell^2}, \tag{5}$$

where τ is the timescale of interest and ℓ is the diffusion length over τ. This yields $\ell = \sqrt{D\tau}$.
In the case of magnetic diffusion, the diffusion constant is the magnetic diffusivity in the post-shock region, ν_M, and the timescale of interest is L/u, the dynamic timescale. The magnetic diffusivity is,

$$\nu_M = \frac{c^2\eta_\perp}{4\pi}, \tag{6}$$

where c is the speed of light, and $\eta_\perp$ is the transverse Spitzer resistivity. The expression for transverse Spitzer resistivity is taken from the *Plasma Formulary*, [18]:

$$\eta_\perp = 1.15\times10^{-14}\frac{Z\ln\Lambda}{T_e^{3/2}}\,\mathrm{sec}, \tag{7}$$

where Z is the ionization, $\ln\Lambda$ is the Coulomb logarithm, and T_e is the electron temperature in eV.
Altogether this yields

$$\ell_M = \sqrt{\frac{\nu_M L}{u}} = \sqrt{\frac{c^2\eta_\perp L}{4\pi u}} \tag{8}$$

4. $0.1 < \beta_{\mathrm{ram}} < 10$. β_{ram} is the ratio of ram pressure of the jet to the magnetic pressure of the field

$$\beta_{\mathrm{ram}} = \frac{\rho u^2}{B^2/8\pi}, \tag{9}$$

where B is magnetic field strength.
A typical accreting young star system with a magnetic field of 1000 G will have $\beta_{\mathrm{ram}} \sim 1$. The range of acceptable β_{ram} imposed here corresponds to magnetic field of 3000 G (low β_{ram}) to 300 G (high β_{ram}).

5. **Re > 10³**. *Re* is the Reynolds number, the ratio of the viscous timescale to the dynamic timescale, Lu/ν_i, where ν_i is the ion viscosity (defined below). Imposing $Re > 10^3$ insures that the viscous smoothing length scale, ℓ_ν, is smaller than all other length scales.
As before $\ell_\nu = \sqrt{D\tau}$. In this case, the diffusion constant, *D*, is the ion viscosity, ν_i, and the timescale of interest, τ is the dynamic timescale, L/u,

$$\ell_\nu = \sqrt{D\tau} = \sqrt{\frac{\nu_i L}{u}} = \frac{L}{\sqrt{Re}}. \tag{10}$$

The ion viscosity, ν_i, was calculated according to

$$\nu_i = \frac{u_{th,i}^2}{\nu_{ii}} = 2\times10^{19}\frac{T_i^{5/2}}{n_i Z^4\sqrt{A}\ln\Lambda}\ \mathrm{cm^2\ s^{-1}}, \tag{11}$$

where $u_{th,\ i}$ and ν_{ii} are the ion thermal velocity and the ion-ion collisional frequency, respectively, and expressions for both were taken from the *Plasma Formulary*, [18]. In the expression for ν_i, T_i is the ion temperature in eV, n_i is the ion density in $\mathrm{cm^{-3}}$, *Z* is the ionization, *A* is the atomic mass, and ln Λ is the Coulomb logarithm.

To have a well-scaled experiment, we need these five criteria to be true at once. For every material, there is some four-dimensional volume in T_e–u–ρ–B space where all five of these criteria are met.

A four dimensional space is difficult to visualize, much less translate into a figure. In order to investigate the parameter space, we held T_e and *B* constant and considered the 2-D u–ρ space, as seen in Fig. 2. In each of the plots in Fig. 2, the shaded area represents the region in u–ρ space where the criterion is not met. Obviously, this area will shift depending on material type, temperature and magnetic field strength. We assumed that the magnetic field is 10 T because this is current capability; from the perspective of the dimensionless number criteria this is no downside to a higher field.

In experimenting with material and temperature, we found that every material has an ideal temperature at which the acceptable area is maximized. (For carbon this ideal temperature is around 60 eV, which is why that is shown in Fig. 2.) Second, both very low-Z and very high-Z materials had smaller acceptable area than medium-Z materials such as carbon. We chose to present carbon because it is a non-toxic, medium-Z material that lends itself readily to target fabrication.

As seen in Fig. 2, the first criterion, Mach number, favors high velocity. The second criterion, collisionality, favors high density, low velocity conditions, because $\lambda_{\mathrm{MFP}} \propto 1/n_i$ and $\lambda_{\mathrm{MFP}} \propto u^4$. The third criterion, magnetic diffusion length, favors high velocity as well because $\ell_M \propto 1/u$. Magnetic diffusion length also favors higher temperatures because $\ell_M \propto 1/T^{3/4}$. The fourth criterion, β_{ram}, favors low density, low velocity conditions because $\beta_{\mathrm{ram}} \propto \rho$ and $\beta_{\mathrm{ram}} \propto u^2$. (As seen in Fig. 2, it is possible for density and velocity to be too low, but the high β_{ram} end of the range is more limiting.) The fifth and final criterion, Reynolds number, favors high velocity, high density conditions because $Re \propto u$ and $\nu_i \propto 1/n_i$. Taken together, these criteria limit the parameter space to an area around $\rho \sim 10^{-6}$–10^{-5} g cm^{-3} and $u \sim 100$–200 km s^{-1} satisfies all five.

Table 1 presents the plasma parameters and calculated length scales and dimensionless numbers for the experimental plasma and the astrophysical system.

3. Experimental considerations

As seen in Fig. 1, our experiment requires an incoming plasma jet (the “accreting flow”) and a surface for it to run into (the “stellar surface”). This paper does not delve into the details of producing a steady carbon plasma jet with $T_e \sim 60$ eV, $\rho \sim 10^{-6}$–10^{-5} g cm^{-3}, and $u \sim 100$–200 km s^{-1}. However, we note that other experimental teams have produced plasma jets made of CH or C, for example Gregory et al. [11] and Kuramitsu et al. [24].

Fig. 3 shows the schematic of one possible experiment, based on the concept used by Gregory et al. [11], which produced jets with $\rho \sim 10^{-4}$ g cm^{-3}, $T_e \sim 10$ eV, and $u \sim 300$ km s^{-1}. In this design, lasers hit the rear side of a thin, conical target (shown in cross section), producing a collimated plasma jet that impacts against a solid block,

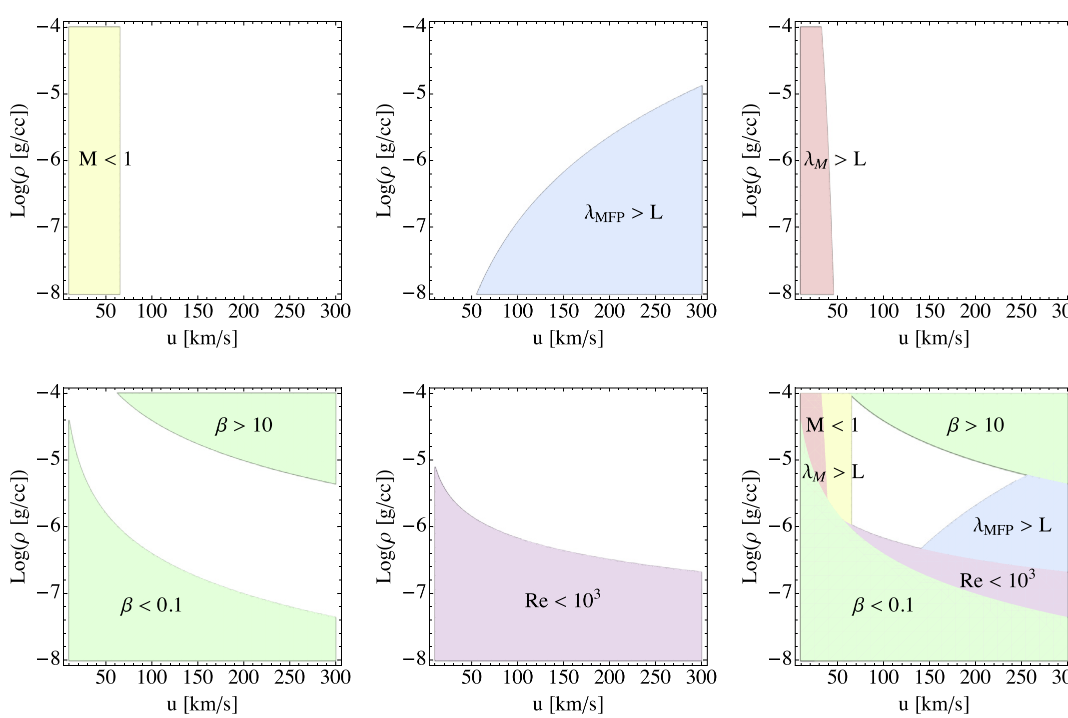

Fig. 2. Criteria region plots for carbon plasma at 60 eV with a 10 T magnetic field. In each plot, the colored area is the region where the conditions is *not* met. Top row, left to right: Mach number, collisionality, and magnetic diffusion length. Bottom row, left to right: ram plasma β, Reynolds number, and all criteria plotted together.

Table 1
A side-by-side comparison of our ideal experimental jets and typical numbers in an accretion stream. The accreting star's plasma parameters are halfway in between those for T Tauri and Herbig Ae/Be stars. For the astrophysical system, velocity was assuming free-fall from the inner edge of the disk, see Calvet and Gullbring [5], Dullemond et al. [7], Hillenbrand et al. [17], Natta et al. [32]. Mass density was calculated from accretion stream energy fluxes found in Calvet and Gullbring [5], Mendigutía et al. [28]. Magnetic field strength was taken from Johns-Krull [19], Johns-Krull et al. [20], Valenti and Johns-Krull [47], Wade et al. [48], Yang et al. [49].

Parameter	Unit	Experiment	Accreting star
Mass density, ρ	g cm^{-3}	5×10^{-6}	2×10^{-11}
Average atomic number	–	6	1.1
Average mass number	–	12	1.3
Average ionization	–	4.9	0.6
Electron density, n_e	cm^{-3}	10^{18}	6×10^{12}
Electron temperature, T_e	eV	60	1
Velocity, u	km s^{-1}	150	450
Magnetic field strength, B	G	10^5	700
Length scale, L	cm	0.1	10^9
Ion collisional MFP, $\lambda_{\mathrm{MFP,\,i}}$	cm	0.03	2×10^6
Magnetic diffusion length, ℓ_M	cm	0.02	200
Viscous smoothing length, ℓ_ν	cm	0.001	5000
Mach number, $\mathcal{M}$	–	2	33
Collisionality, $\lambda_{\mathrm{MFP,\,i}}/L$	–	0.3	0.002
Magnetic diffusion length ratio, λ_M/L	–	0.1	2×10^{-7}
Ram plasma beta, β_{ram}	–	3	1
Reynolds number, Re	–	10^5	10^{10}
Magnetic Reynolds number, Re$_m$	–	20	10^{10}

producing shock structures for us to study. A magnetic field parallel to the direction of jet flow is imposed on the entire experiment.

Regardless of how the plasma jet is produced, the primary diagnostics for this experiment would be proton radiography, self-emission visible light imaging, and perhaps imaging Thomson scattering.

Imaging the experiment in self-emitted visible/UV light would reveal the highest temperature structures because they would glow brightest. (The opacity is too low for X-ray radiography to reveal mass density.) We would hope to see the bright shock front.

Likewise, proton radiography can be used to image magnetic field structures. Conceptually, proton radiography is similar to more traditional X-ray radiography. A source generates protons (analogous to the X-rays), which pass through the experiment and strike piece of plastic (analagous to X-ray film). We intend to use a monoenergetic-proton radiography technique described in Li et al. [26,27]. A capsule of deuterium-helium-3 is imploded with high-intensity lasers, generating a burst of 14.7 MeV and 3.6 MeV protons. These protons pass through the experiment and strike a piece of CR-39, a clear plastic nuclear track detector, leaving a trail of broken bonds in the plastic that can be developed as an image when the plastic is etched.

It might be possible to use Thomson scattering to ascertain plasma parameters. The geometry of the experiment (a jet hitting a solid block) makes Thomson scattering inherently complicated. But it might be possible to bring the probe beam in the side and use imaging Thomson scattering in a transverse direction (that is, perpendicular to the jet flow direction) [40]. This would tell us whether the edges of the shock (that is, the splash zone) are cooler and less dense that the central region, which would tie into the questions from Section 1.

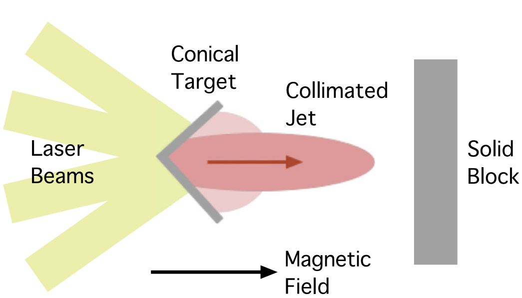

Fig. 3. Schematic diagram of the experiment. Rear-irradiation launches a plasma jet toward a solid block along a parallel imposed magnetic field.

4. Conclusions

To establish the connection between a typical accreting star system and the lab, we imposed five criteria on the dimensionless numbers that underly both systems:

1. $\mathcal{M} > \mathbf{1}$ where $\mathcal{M}$ is the Mach number.
2. $\lambda_{\mathrm{MFP}} < \boldsymbol{L}$ where λ_{MFP} is the ratio of the ion-ion mean free path.
3. $\ell_{\boldsymbol{M}} < \boldsymbol{L}$ where ℓ_M is the magnetic diffusion lengthscale.
4. $\mathbf{0.1} < \boldsymbol{\beta}_{\mathrm{ram}} < \mathbf{10}$ where β_{ram} is the ratio of ram pressure of the jet to the magnetic pressure of the field.
5. $\mathbf{Re} > \mathbf{10^3}$ where Re is the Reynolds number.

We find a region in parameter space where all five criteria are satisfied: a carbon plasma jet with $T_e \sim 60$ eV, $\rho \sim 10^{-6}$–10^{-5} g cm^{-3} and $u \sim 100$–200 km s^{-1} with an imposed field of $B \sim 10$ T. Such an experiment would represent an average accretion stream onto a pre-main sequence star with $B \sim 700$ G. (Of course, scaling accretion streams onto young stars with *lower* magnetic fields is easily accomplished; we can always lower the imposed experimental field.)

At 700 G, we are above maximum expected magnetic field on a Herbig Ae/Be star, usually expected to be a few hundred Gauss [48], but right at the minimum field for a T Tauri star, which have measured fields of several kG [19,20,47,49]. To recreate the conditions on a $B = 2000$ G star, we need $\beta_{\mathrm{ram}} = 0.3$, which requires $B \sim 30$ T, something outside the current capabilities. However, improvements in magnetic field generation could open up this experimental regime.

Acknowledgments

This work is funded by the U.S. Department of Energy, through the NNSA-DS and SC-OFES Joint Program in High-Energy-Density Laboratory Plasmas, grant number DE-NA0002956, and the National Laser User Facility Program, grant numbers DE-NA0002719 and R19071, and through the Laboratory for Laser Energetics, University of Rochester by the NNSA/OICF under Cooperative Agreement No. DE-NA0001944.

We thank Nuria Calvet for enlightening discussions on magnetospheric accretion and accretion shock models.

References

[1] C. Argiroffi, E. Flaccomio, J. Bouvier, J.-F. Donati, K.V. Getman, S.G. Gregory, G.A.J. Hussain, M.M. Jardine, M.B. Skelly, F.M. Walter, Variable X-ray emission from the accretion shock in the classical T Tauri star V2129 Ophiuchi, A&A 530 (2011) A1, doi: 10.1051/0004-6361/201016321.
[2] C. Argiroffi, A. Maggio, G. Peres, X-ray emission from MP Muscae: an old classical T Tauri star, A&A 465 (2007) L5–L8, doi: 10.1051/0004-6361:20067016.
[3] J. Bouvier, S.H.P. Alencar, T.J. Harries, C.M. Johns-Krull, M.M. Romanova, Magnetospheric accretion in classical T Tauri stars, Protostars Planets V (2007) 479–494.
[4] N.S. Brickhouse, S.R. Cranmer, A.K. Dupree, G.J.M. Luna, S. Wolk, A Deep Chandra X-ray spectrum of the accreting young star TW Hydrae, ApJ 710 (2010) 1835–1847, doi: 10.1088/0004-637X/710/2/1835.
[5] N. Calvet, E. Gullbring, The structure and emission of the accretion shock in T Tauri stars, ApJ 509 (1998) 802–818, doi: 10.1086/306527.
[6] J.J. Drake, J. Braithwaite, V. Kashyap, H.M. Günther, N.J. Wright, Burn out or fade away? On the X-ray and magnetic death of intermediate mass stars, ApJ 786 (2014) 136, doi: 10.1088/0004-637X/786/2/136.
[7] C.P. Dullemond, C. Dominik, A. Natta, Passive irradiated circumstellar disks with an inner hole, ApJ 560 (2001) 957–969, doi: 10.1086/323057.
[8] P. Ghosh, F.K. Lamb, Accretion by rotating magnetic neutron stars. II - radial and vertical structure of the transition zone in disk accretion, ApJ 232 (1979) 259–276, doi: 10.1086/157285.
[9] P. Ghosh, F.K. Lamb, Accretion by rotating magnetic neutron stars. III - accretion torques and period changes in pulsating X-ray sources, ApJ 234 (1979) 296–316, doi: 10.1086/157498.

[10] C.A. Grady, K. Hamaguchi, G. Schneider, B. Stecklum, B.E. Woodgate, J.E. McCleary, G.M. Williger, M.L. Sitko, F. Ménard, T. Henning, S. Brittain, M. Troutmann, B. Donehew, D. Hines, J.P. Wisniewski, D.K. Lynch, R.W. Russell, R.J. Rudy, A.N. Day, A. Shenoy, D. Wilner, M. Silverstone, J.-C. Bouret, H. Meusinger, M. Clampin, S. Kim, R. Petre, M. Sahu, M. Endres, K.A. Collins, Locating the accretion footprint on a Herbig Ae star: MWC 480, ApJ 719 (2010) 1565–1581, doi: 10.1088/0004-637X/719/2/1565.
[11] C.D. Gregory, J. Howe, B. Loupias, S. Myers, M.M. Notley, Y. Sakawa, A. Oya, R. Kodama, M. Koenig, N.C. Woolsey, Astrophysical jet experiments with colliding laser-produced plasmas, ApJ 676 (2008) 420–426, doi: 10.1086/527352.
[12] V.P. Grinin, O.V. Kozlova, A. Natta, I. Ilyin, I. Tuominen, A.N. Rostopchina, D.N. Shakhovskoy, Optical spectra of five UX Orionis-type stars, A&A 379 (2001) 482–495, doi: 10.1051/0004-6361:20011280.
[13] H.M. Günther, C. Liefke, J.H.M.M. Schmitt, J. Robrade, J.-U. Ness, X-ray accretion signatures in the close CTTS binary V4046 Sagittarii, A&A 459 (2006) L29–L32, doi: 10.1051/0004-6361:20066306.
[14] P. Hartigan, J.M. Foster, B.H. Wilde, R.F. Coker, P.A. Rosen, J.F. Hansen, B.E. Blue, R.J.R. Williams, R. Carver, A. Frank, Laboratory experiments, numerical simulations, and astronomical observations of deflected supersonic jets: application to HH 110, ApJ 705 (2009) 1073–1094, doi: 10.1088/0004-637X/705/1/1073.
[15] P. Hartigan, S.J. Kenyon, L. Hartmann, S.E. Strom, S. Edwards, A.D. Welty, J. Stauffer, Optical excess emission in T Tauri stars, ApJ 382 (1991) 617–635, doi: 10.1086/170749.
[16] L. Hartmann, N. Calvet, E. Gullbring, P. D'Alessio, Accretion and the evolution of T Tauri disks, ApJ 495 (1998) 385, doi: 10.1086/305277.
[17] L.A. Hillenbrand, S.E. Strom, F.J. Vrba, J. Keene, Herbig Ae/Be stars - intermediate-mass stars surrounded by massive circumstellar accretion disks, ApJ 397 (1992) 613–643, doi: 10.1086/171819.
[18] J.D. Huba, U. States., N.R.L.U.S. , NRL Plasma Formulary, Naval Research Laboratory], [Washington, DC, 2009.
[19] C.M. Johns-Krull, The magnetic fields of classical T Tauri stars, ApJ 664 (2007) 975–985, doi: 10.1086/519017.
[20] C.M. Johns-Krull, J.A. Valenti, C. Koresko, Measuring the magnetic field on the classical T Tauri star BP Tauri, ApJ 516 (1999) 900–915, doi: 10.1086/307128.
[21] J.H. Kastner, D.P. Huenemoerder, N.S. Schulz, C.R. Canizares, D.A. Weintraub, Evidence for accretion: high-Resolution X-ray spectroscopy of the classical T Tauri star TW Hydrae, ApJ 567 (2002) 434–440, doi: 10.1086/338419.
[22] A. Königl, Disk accretion onto magnetic T Tauri stars, ApJ 370 (1991) L39–L43, doi: 10.1086/185972.
[23] C.M. Krauland, R.P. Drake, C.C. Kuranz, B. Loupias, T. Plewa, C.M. Huntington, D.N. Kaczala, S. Klein, R. Sweeney, R.P. Young, E. Falize, B. Villette, P.A. Keiter, Reverse radiative shock laser experiments relevant to accreting stream-disk impact in interacting binaries, ApJ 762 (2013) L2, doi: 10.1088/2041-8205/762/1/L2.
[24] Y. Kuramitsu, Y. Sakawa, J.N. Waugh, C.D. Gregory, T. Morita, S. Dono, H. Aoki, H. Tanji, B. Loupias, M. Koenig, N. Woolsey, H. Takabe, Jet formation in counterstreaming collisionless plasmas, ApJ 707 (2009) L137–L141, doi: 10.1088/0004-637X/707/2/L137.
[25] C.C. Kuranz, R.P. Drake, E.C. Harding, M.J. Grosskopf, H.F. Robey, B.A. Remington, M.J. Edwards, A.R. Miles, T.S. Perry, B.E. Blue, T. Plewa, N.C. Hearn, J.P. Knauer, D. Arnett, D.R. Leibrandt, Two-dimensional blast-wave-driven Rayleigh−Taylor instability: experiment and simulation, ApJ 696 (2009) 749–759, doi: 10.1088/0004-637X/696/1/749.
[26] C.K. Li, F.H. Séguin, J.A. Frenje, J.R. Rygg, R.D. Petrasso, R.P.J. Town, P.A. Amendt, S.P. Hatchett, O.L. Landen, A.J. MacKinnon, P.K. Patel, V.A. Smalyuk, T.C. Sangster, J.P. Knauer, Measuring E and B fields in laser-produced plasmas with monoenergetic proton radiography, Phys. Rev. Lett. 97 (13) (2006) 135003, doi: 10.1103/PhysRevLett.97.135003.
[27] C.K. Li, F.H. Séguin, J.A. Frenje, J.R. Rygg, R.D. Petrasso, R.P.J. Town, O.L. Landen, J.P. Knauer, V.A. Smalyuk, Observation of Megagauss-field topology changes due to magnetic reconnection in laser-produced plasmas, Phys. Rev. Lett. 99 (5) (2007) 055001, doi: 10.1103/PhysRevLett.99.055001.
[28] I. Mendigutía, N. Calvet, B. Montesinos, A. Mora, J. Muzerolle, C. Eiroa, R.D. Oudmaijer, B. Merín, Accretion rates and accretion tracers of Herbig Ae/Be stars, A&A 535 (2011) A99, doi: 10.1051/0004-6361/201117444.
[29] J. Muzerolle, P. D'Alessio, N. Calvet, L. Hartmann, Magnetospheres and disk accretion in Herbig Ae/Be stars, ApJ 617 (2004) 406–417, doi: 10.1086/425260.
[30] J. Muzerolle, K.L. Luhman, C. Briceño, L. Hartmann, N. Calvet, Measuring accretion in young substellar objects: approaching the planetary mass regime, ApJ 625 (2005) 906–912, doi: 10.1086/429483.
[31] A. Natta, V.P. Grinin, L.V. Tambovtseva, An interesting episode of accretion activity in UX Orionis, ApJ 542 (2000) 421–427, doi: 10.1086/309526.
[32] A. Natta, T. Prusti, R. Neri, D. Wooden, V.P. Grinin, V. Mannings, A reconsideration of disk properties in Herbig Ae stars, A&A 371 (2001) 186–197, doi: 10.1051/0004-6361:20010334.
[33] A. Natta, L. Testi, S. Randich, Accretion in the ρ-Ophiuchi pre-main sequence stars, A&A 452 (2006) 245–252, doi: 10.1051/0004-6361:20054706.
[34] S. Orlando, G.G. Sacco, C. Argiroffi, F. Reale, G. Peres, A. Maggio, X-Ray emitting MHD accretion shocks in classical T Tauri stars. Case for moderate to high plasma-β values, A&A 510 (2010) A71, doi: 10.1051/0004-6361/200913565.
[35] H.-S. Park, D.D. Ryutov, J.S. Ross, N.L. Kugland, S.H. Glenzer, C. Plechaty, S.M. Pollaine, B.A. Remington, A. Spitkovsky, L. Gargate, G. Gregori, A. Bell, C. Murphy, Y. Sakawa, Y. Kuramitsu, T. Morita, H. Takabe, D.H. Froula, G. Fiksel, F. Miniati, M. Koenig, A. Ravasio, A. Pelka, E. Liang, N. Woolsey, C.C. Kuranz, R.P. Drake, M.J. Grosskopf, Studying astrophysical collisionless shocks with counterstreaming plasmas from high power lasers, High Energy Density Phys. 8 (2012) 38–45, doi: 10.1016/j.hedp.2011.11.001.
[36] B.A. Remington, R.P. Drake, D.D. Ryutov, Experimental astrophysics with high power lasers and Z pinches, Rev. Mod. Phys. 78 (2006) 755–807, doi: 10.1103/RevModPhys.78.755.
[37] B.A. Remington, R.P. Drake, H. Takabe, D. Arnett, A review of astrophysics experiments on intense lasers, Phys. Plasmas 7 (2000) 1641–1652, doi: 10.1063/1.874046.
[38] J. Robrade, J.H.M.M. Schmitt, X-rays from RU Lupi: accretion and winds in classical T Tauri stars, A&A 473 (2007) 229–238, doi: 10.1051/0004-6361:20077644.
[39] M.M. Romanova, G.V. Ustyugova, A.V. Koldoba, R.V.E. Lovelace, Three-dimensional simulations of disk accretion to an inclined dipole. II. Hot spots and variability, ApJ 610 (2004) 920–932, doi: 10.1086/421867.
[40] J.S. Ross, D.H. Froula, A.J. Mackinnon, C. Sorce, N. Meezan, S.H. Glenzer, W. Armstrong, R. Bahr, R. Huff, K. Thorp, Implementation of imaging Thomson scattering on the Omega laser, Rev. Sci. Instrum. 77 (10) (2006) 100000, doi: 10.1063/1.2220077.
[41] D. Ryutov, R.P. Drake, J. Kane, E. Liang, B.A. Remington, W.M. Wood-Vasey, Similarity criteria for the laboratory simulation of Supernova hydrodynamics, ApJ 518 (1999) 821–832, doi: 10.1086/307293.
[42] J.H.M.M. Schmitt, J. Robrade, J.-U. Ness, F. Favata, B. Stelzer, X-rays from accretion shocks in T Tauri stars: the case of BP Tau, A&A 432 (2005) L35–L38, doi: 10.1051/0004-6361:200500014.
[43] B. Stelzer, J.H.M.M. Schmitt, X-ray emission from a metal depleted accretion shock onto the classical T Tauri star TW Hya, A&A 418 (2004) 687–697, doi: 10.1051/0004-6361:20040041.
[44] D.A. Swartz, J.J. Drake, R.F. Elsner, K.K. Ghosh, C.A. Grady, E. Wassell, B.E. Woodgate, R.A. Kimble, The Herbig Ae Star HD 163296 in X-rays, ApJ 628 (2005) 811–816, doi: 10.1086/429984.
[45] P. Testa, D.P. Huenemoerder, N.S. Schulz, K. Ishibashi, X-ray emission from young stellar objects in the ϵChamaeleontis group: the Herbig Ae star HD 104237 and associated low-Mass stars, ApJ 687 (2008) 579–597, doi: 10.1086/591485.
[46] J.A. Valenti, G. Basri, C.M. Johns, T Tauri stars in blue, AJ 106 (1993) 2024–2050, doi: 10.1086/116783.
[47] J.A. Valenti, C.M. Johns-Krull, Observations of magnetic fields on T Tauri stars, Ap&SS 292 (2004) 619–629, doi: 10.1023/B:ASTR.0000045068.34836.cf.
[48] G.A. Wade, S. Bagnulo, D. Drouin, J.D. Landstreet, D. Monin, A search for strong, ordered magnetic fields in Herbig Ae/Be stars, MNRAS 376 (2007) 1145–1161, doi: 10.1111/j.1365-2966.2007.11495.x.
[49] H. Yang, C.M. Johns-Krull, J.A. Valenti, Measuring the magnetic field of the classical T Tauri star TW Hydrae, ApJ 635 (2005) 466–475, doi: 10.1086/497070.